www.czasopisma.pan.pl PAN POLSKA AKADEMIA NAUK www.journals.pan.pl

Arch. Metall. Mater. **67** (2022), 2, 471-478

DOI: https://doi.org/10.24425/amm.2022.137779

R. GAWEL[1*], Ł. ROGAL[2], K. PRZYBYLSKI[1], KENJI MATSUDA[3]

INFLUENCE OF HIGH-TEMPERATURE OXIDIZING CONDITIONS ON ALCOCRCUNI HIGH ENTROPY ALLOYS WITH AND WITHOUT SILICON ADDITION

Initial investigations on oxidation behaviour and phase transformations of equimolar AlCoCrCuNi high entropy alloy with and without 1 at.% silicon addition during 24-hr exposure to air atmosphere at 1273 K was carried out in this work. After determining the oxidation kinetics of the samples by means of thermogravimetric analysis, the morphology, chemical and phase compositions of the oxidized alloys were determined by means of scanning electron microscopy, energy dispersive X-ray spectroscopy and X-ray diffraction analysis. Additional cross-section studies were performed using transmission electron microscopy combined with energy dispersive X-ray spectroscopy and selected area electron diffraction. From all these investigations, it can be concluded that minor silicon addition improves the oxidation kinetics and hinders the formation of an additional FCC structure near the surface of the material.

Keywords: high entropy alloys; high temperature oxidation; phase analysis; alloying element

1. Introduction

Up to now, traditional alloys have met industrial requirements for structural applications. However, due to constantly increasing demands, implementation of alternative materials, e.g. high entropy alloys (HEAs), has been considered. These metallic systems can be defined as alloys that consist of five or more principle elements in amounts that range between 5 and 35%at. [1], or exhibit configurational entropy (ΔS_{conf}) $\geq 1.5R$ (R – universal gas constant) [2]. The configurational entropy of the multi-principle element alloy can be calculated from the following equation:

$$\Delta S_{conf} = -R\Sigma X_i \ln X_i \tag{1}$$

where X_i – atom fraction of principle element i.

These multi-principle element materials are usually built of a face centered cubic (FCC) or body centered cubic (BCC) crystalline structure, in contrast to the intermetallic phases that constitute traditional alloys. High entropy alloys based on an FCC phase demonstrate relatively good ductility [3,4], whereas BCC-based HEAs are characterized by great hardness and compressive strength [1,5]. Some element combinations also allow for obtaining alloys that consist of both FCC and BCC structures [1,6-8]. For example, in specific aluminium concentration ranges, Al_xCoCrFeNi, Al_xCoCrCuFeNi and Al_xCoCrFeMnNi systems become dual FCC/BCC phase materials [1,6-8]. Such multi-principle element alloys can also be classified as high entropy alloys, as long as the above-mentioned thermodynamic condition is met. Both structures in the aforementioned dual phase alloys contribute to their mechanical properties. For example, studies have shown that, as Al content and subsequently the percentage of the BCC phase in the Al_xCoCrFeMnNi HEA system increases, the ductility of the material decreases and its hardness and compressive strength increase [8]. It was additionally determined that incorporating silicon into AlCoCrFeNi and AlCoCrCuFeNi high entropy alloy systems also leads to an increase in material hardness and compressive mechanical properties [9,10]. Unfortunately, large amounts of Si in the systems result in the formation of additional phases that contribute to the embrittlement of the alloys [9,10]. Therefore, it is important not to exceed a certain molar ratio of Si in a given HEA.

While Al_xCoCrFeNi and Al_xCoCrCuFeNi systems have been comprehensively studied for several years, equimolar AlCoCrCuNi high entropy alloys have not been as thoroughly

[1] AGH UNIVERSITY OF SCIENCE AND TECHNOLOGY, FACULTY OF MATERIALS SCIENCE AND CERAMICS, DEPARTMENT OF PHYSICAL CHEMISTRY AND MODELLING, AL. MICKIEWICZA 30, 30 -059 KRAKÓW, POLAND
[2] POLISH ACADEMY OF SCIENCES, INSTITUTE OF METALLURGY AND MATERIALS, 25 REYMONTA STR., 30-059 KRAKOW POLAND
[3] UNIVERSITY OF TOYAMA, FACULTY OF SUSTAINABLE DESIGN, DEPARTMENT OF MATERIALS DESIGN AND ENGINEERING, 3190 GOFUKU, TOYAMA 930-8555, JAPAN
* Corresponding author: ragaw@agh.edu.pl

investigated. This HEA composition was initially studied by Hsu et al. [11], who determined that the material consisted of a Cu-rich FCC interdendrite phase and a dendrite region containing a BCC and B2-ordered BCC structure built of the constituent elements with reduced copper concentration. Further research on AlCoCrCuNi high entropy alloy, performed years later by Rogal et al. [12,13], demonstrated that exposure to temperatures above 873 K can lead to the formation of a tetragonal sigma phase inside the material, which simultaneously contributes to material hardness and embrittlement [14,15].

Up to now, oxidation studies have been carried out in air at 1273 K and even at a higher temperature (1323 K) on several similar HEA compositions, such as $Al_xCoCrFeNi$, $Al_{20}Cr_{25}Co_{25}Ni_{25}Si_5$, $Al_xCoCrCuFeNi$ and $AlCoCrCu_xFeNi$ [16-19]. After each material was subjected to a respective oxidation process, protective scales consisting of Cr_2O_3 and Al_2O_3, or simply pure Al_2O_3 were observed on their surfaces, thereby providing protection against further oxidation [16-19]. Taking this into account, it is our opinion that the oxidation behaviour of equimolar AlCoCrCuNi and AlCoCrCuNi with minor silicon addition should also be researched at such a high temperature (1273 K) in order to determine whether similar results can be achieved. Furthermore, if these materials prove to be resistant against oxidation at such a high temperature, then they also show some promise for practical applications at lower temperatures.

The goal of this work is to present the results of initial studies on the AlCoCrCuNi phase composition after exposure to high-temperature oxidizing operating conditions and to determine whether adding silicon to the investigated system can have a beneficial effect on its structure and oxidation resistance. If so, this would provide an avenue for future research involving incorporation of Si at different concentrations into the HEA system in order to determine the optimum silicon content for improving AlCoCrCuNi structural and corrosion-resistant properties at elevated temperatures.

2. Experimental

AlCoCrCuNi materials with and without 1 at.% Si were synthesized from elements of 99.99 wt.% purity in an arc melting furnace with a water-cooled copper plate under protective argon atmosphere. Details of the procedure can be found in [20]. A precision saw was then used to prepare samples in the shape of discs with ~1 cm diameter and ~1.5 mm thickness. These discs were then ground with SiC paper with gradations from 80 to 1000, polished to mirror shine using diamond pastes (9, 3 and then 1 μm) and subsequently cleaned in ethanol.

After these preparations, the materials were oxidized in a thermogravimetric apparatus in air atmosphere at 1273 K for 24 h. The mass changes during the oxidation processes were registered as a function of time by a CI Precision Mk2 microbalance with 0.1 μg sensitivity and 1 μg accuracy. The physicochemical properties of the samples listed in Table 1 were investigated before and after 24-hr exposure to air. These studies include scanning electron microscopy (SEM; HITACHI S-3500N Variable Pressure Scanning Electron Microscope) with an accelerating voltage of 10 kV and 20 μA emission current, electron probe microanalysis (EPMA; JEOL JXA-8230T Electron Probe Microanalyzer), and X-ray diffraction (XRD; Philips PW 1710 diffractometer) with an applied voltage of 30kV and 30mA current performed on the surface of the materials. EPMA investigations were carried out both at selected points and wide areas. XRD was performed using a diffractometer with CoKα filtered radiation. Scans with ±0.1° precision were carried out with a step size of 0.05° and a rate of 1° every 10 min. Thin cross-sections of the samples were also prepared by means of the focused ion beam (FIB; Hitachi FB-2000A FIB) method and subsequently placed on a molybdenum mesh. The cross-sections were then subjected to transmission electron microscopy (TEM; TOPCON EM-002B Transmission Electron Microscope) at 400kV accelerating voltage and 100 mA electron beam current combined with energy dispersive X-ray spectroscopy (EDS; Noran Instruments Energy Dispersive X-ray Spectrometer MODEL 623M-3SPT) and selected area electron diffraction (SAED) analysis.

3. Results

The nominal chemical compositions of the obtained multi-principle element alloys are listed in Table 1, along with the configurational entropy values calculated using the formula in eq. (1). From these entropy values it follows that the studied compositions can be classified as high entropy alloys, according to the thermodynamic definition provided by Miracle et al. [2].

TABLE 1

Designation, chemical composition and configurational entropy of samples investigated in this work

Designation	Nominal chemical composition [%at.]						Configurational entropy
	Al	Co	Cr	Cu	Ni	Si	
AlCoCrCuNi	20	20	20	20	20	0	1.61R
AlCoCrCuNi1Si	20	20	20	19	20	1	1.65R

Figure 1 illustrates an XRD pattern obtained from analysing the AlCoCrCuNi1Si sample before exposure to high-temperature conditions. The results indicate that the material consists of both a BCC and an FCC structure without any additional undesired intermetallic phases. The observed peaks correspond with the peaks pertaining to the respective BCC and FCC phases determined from XRD analysis of equimolar AlCoCrCuNi alloys in previous works [11-13], which provide the necessary information on the phase composition of that material in this work as well. According to XRD and TEM studies presented in those papers [11-13], an additional B2 phase was observed along with disordered BCC and FCC structures. However, there is no evidence in the studies presented in this work to confirm the presence of the B2 phase in the AlCoCrCuNi1Si material.

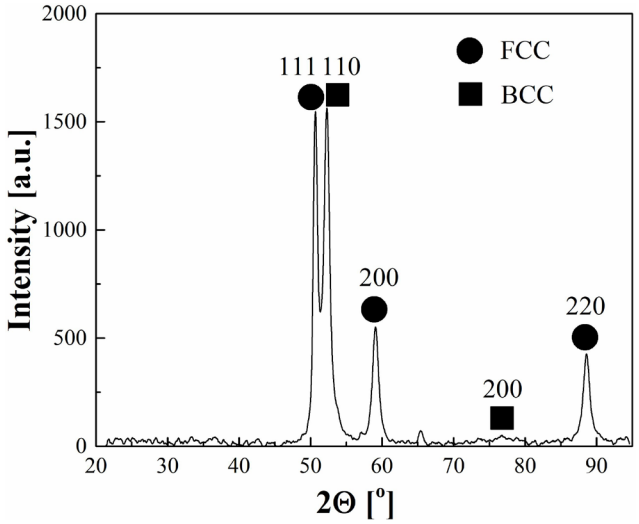

Fig. 1. XRD results obtained from the AlCoCrCuNi1Si high entropy alloy before exposure to high-temperature oxidizing conditions

EPMA wide-area investigations, illustrated in Fig. 2, demonstrate that the material consists of a copper-rich interdendrite region, whereas high concentrations of the remaining elements, including the majority of silicon in the sample, can be found in the dendrite areas. This is also in accordance with phase composition, morphology and chemical composition analysis results presented for equimolar AlCoCrCuNi in literature [11-13], which confirms the tendency of copper to separate itself from other elements in such a HEA system, forming an FCC-structured interdendrite region. It is also interesting to notice that higher concentrations of Al and Ni are located near the dendrite/interdendrite interface. The reason for this is unknown and can be the subject of further studies.

Oxidation kinetics obtained during oxidation of both materials are illustrated in Fig. 3. The curves demonstrate that the mass gain in the case of the AlCoCrCuNi sample is greater than that determined for AlCoCrCuNi1Si, indicating that the silicon-containing material exhibits better oxidation resistance. Unfortunately, it is difficult to determine parabolic rate constants for the oxidation of the alloys, because the mass increase is not continuous as mass losses are also observed throughout the process, especially in the case of AlCoCrCuNi. This phenomenon indicates that, along with scale growth, partial oxide spallation also takes place during the high-temperature oxidation procedure. This spallation is especially noticeable after 4 hours in the case of the sample without Si. After the thermogravimetric analysis was finished, spalled off fragments of the scales from each studied sample were observed in the reaction chamber. This is consistent with the poor scale/substrate adherence observed for a similar

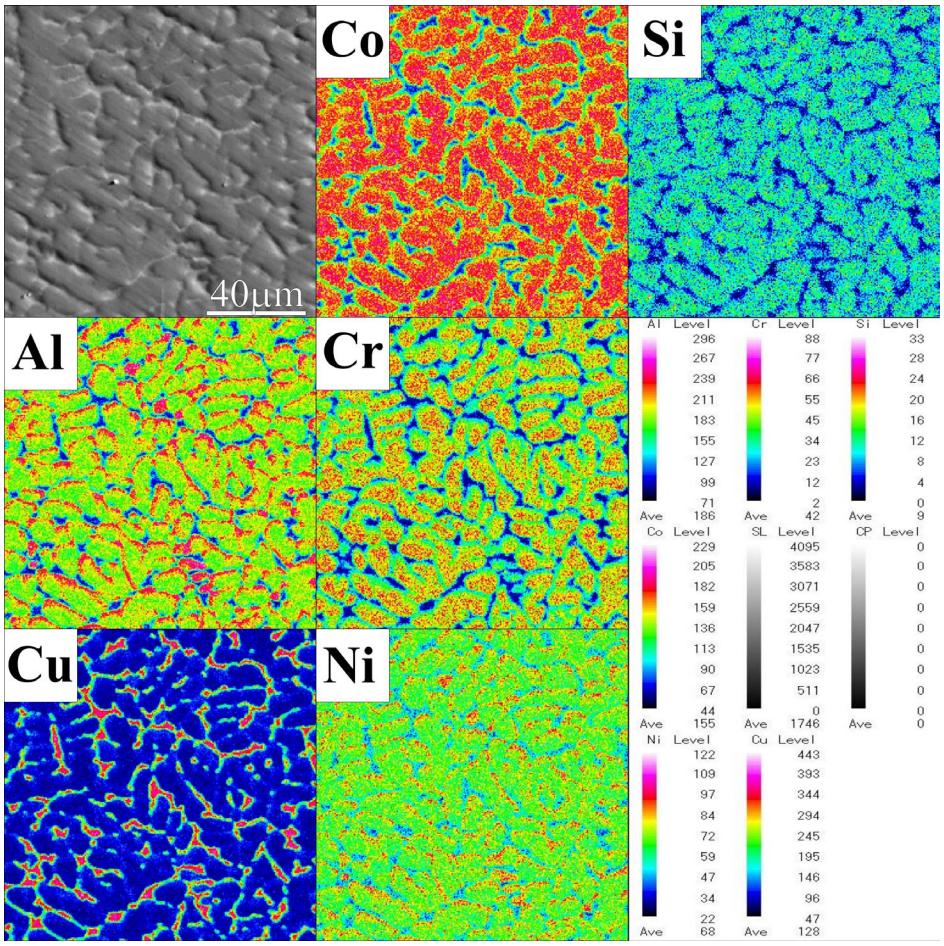

Fig. 2. Secondary electron image and map of elements determined by EPMA wide-area studies performed on the surface of AlCoCrCuNi1Si high entropy alloy before exposure to high-temperature oxidizing conditions

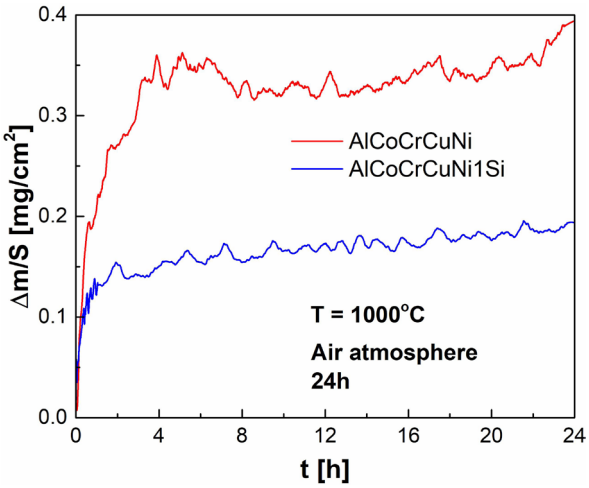

Fig. 3. Mass change per unit area of both AlCoCrCuNi and AlCoCrCuNi1Si as a function of time during oxidation at 1273 K in air atmosphere for 24 h

HEA at 1273 K [19]. As a result, protective scales were found only on certain sections of the AlCoCrCuNi and AlCoCrCuNi1Si alloy surfaces after the oxidation process, as shown in Fig. 4a and Fig. 4b, respectively.

EPMA analysis of a selected area, illustrated in Fig. 5, suggests that Al_2O_3 grows on the AlCoCrCuNi1Si sample during exposure to high-temperature oxidizing conditions. Additionally, some amounts of silicon are determined at certain locations on the surface of the material. On the other hand, Cr and Co can be found throughout the non-oxide protected section surrounded by a Cu-rich interdendrite region.

As for the oxidized AlCoCrCuNi sample, EPMA studies (Fig. 6) confirm that the layer grown on the surface of this sample is also an Al_2O_3 oxide scale. Furthermore, the figure demonstrates that, in this case, mainly Co, along with Cr and Ni, constitutes the dendrite region, whereas Cu remains segregated in the interdendrite areas.

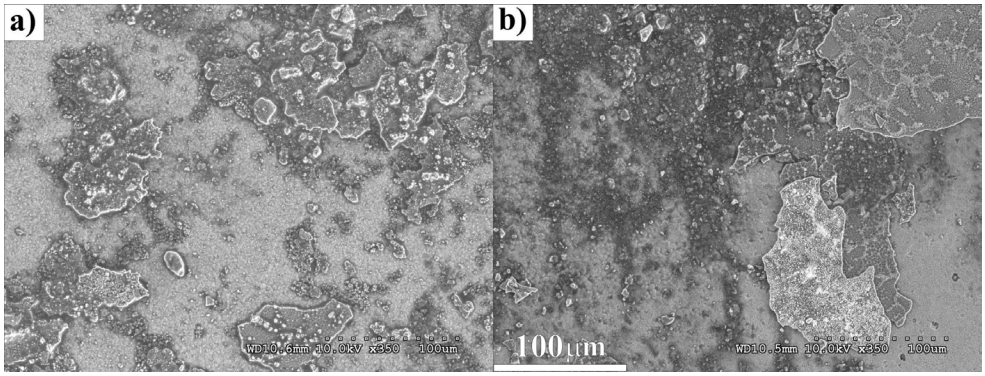

Fig. 4. SEM microphotographs of a) AlCoCrCuNi and b) AlCoCrCuNi1Si high entropy alloys after 24-hr oxidation in air at 1273 K

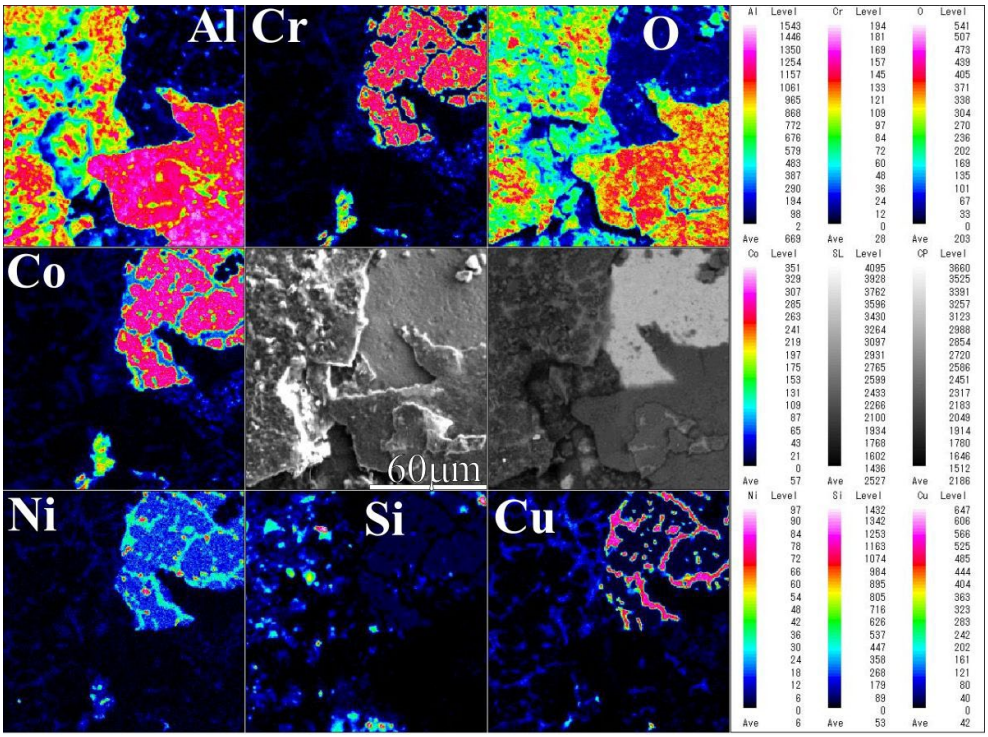

Fig. 5. Secondary electron image, back scattered image, and map of elements determined by EPMA wide-area studies performed on the surface of AlCoCrCuNi1Si high entropy alloy after 24-hr oxidation in air at 1273 K

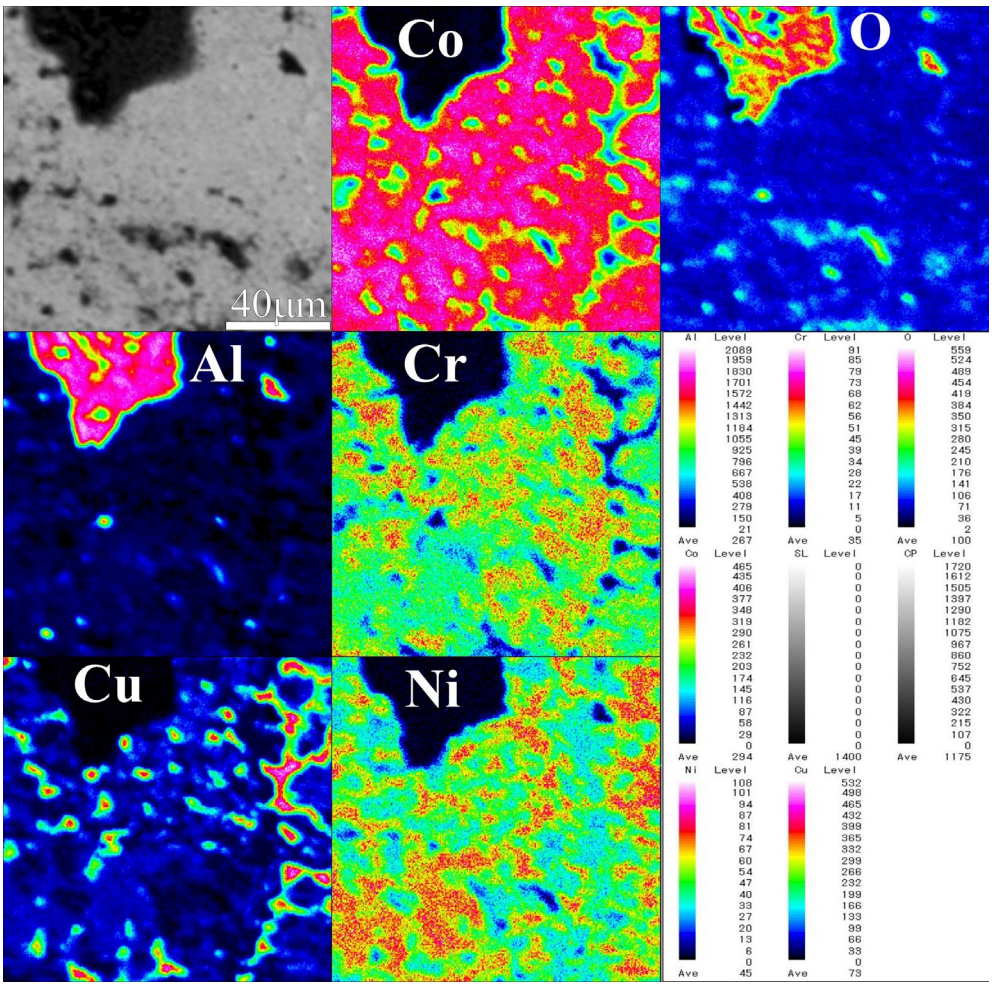

Fig. 6. Back scattered image and map of elements determined by EPMA wide-area studies performed on the surface of AlCoCrCuNi high entropy alloy after 24-hr oxidation in air at 1273 K

Combined TEM-SAED analysis performed on a FIB-prepared cross-section of AlCoCrCuNi after oxidation, illustrated in Fig. 7, indicates that an FCC structure can be found in the vicinity of the Al_2O_3 scale. Next to this structure, another FCC phase can be observed. EDS analysis of points 1 and 2 in Fig. 7, shown in Fig. 8a and Fig. 8b, respectively, reveals that the FCC structure designated as point 1 consists of significant amounts of Co, Cr and Ni. The other is a Cu-rich phase. The molybdenum peak in the EDS patterns can be attributed to the mesh on which the samples were placed.

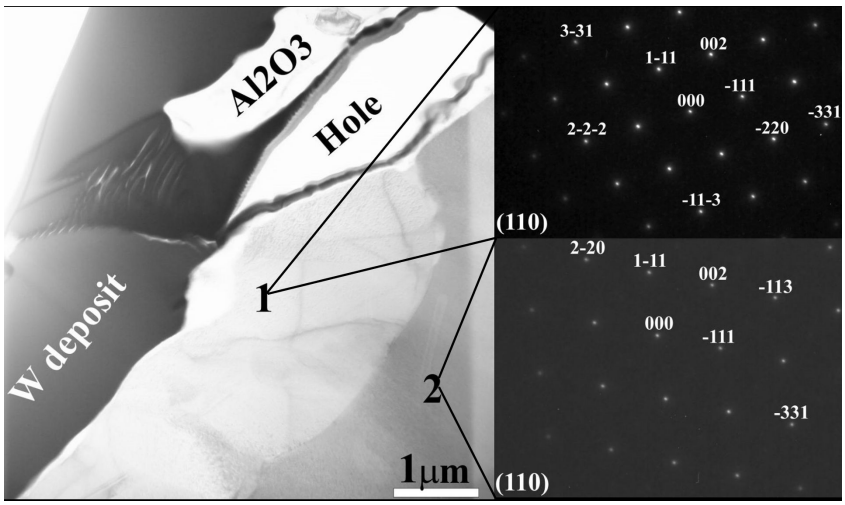

Fig. 7. TEM cross-section image of AlCoCrCuNi after oxidation at 1273 K in air for 24 h combined with SAED patterns obtained from point 1 and point 2 of the microphotograph

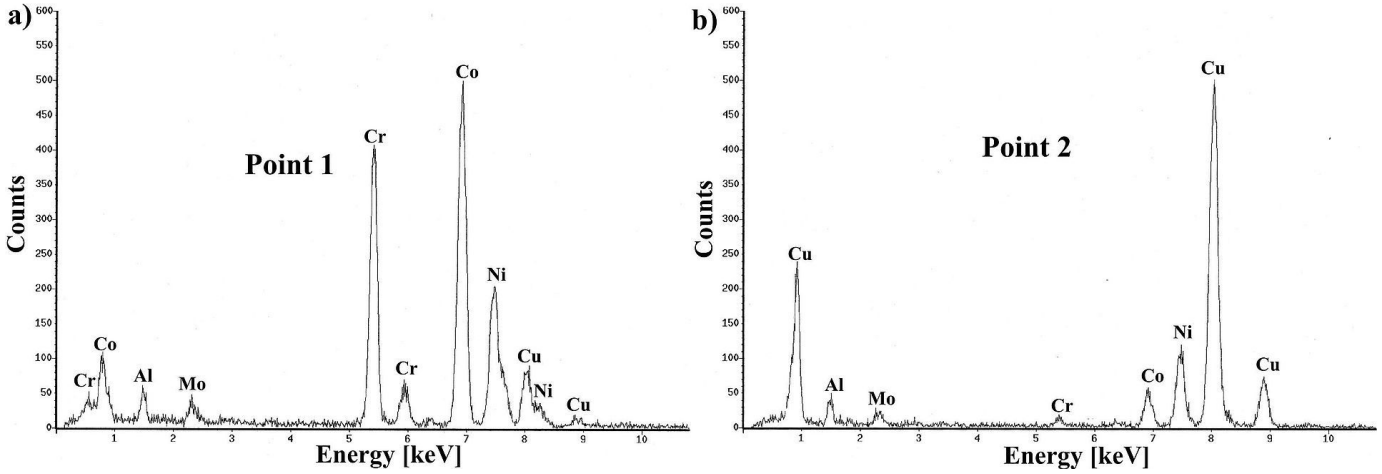

Fig. 8. EDS point analysis obtained from a) point 1 and b) point 2 of the TEM cross-section image of AlCoCrCuNi after oxidation at 1273 K in air for 24 h

Conversely, the phase detected at the microstructure below the Al_2O_3 scale illustrated in Fig. 9 was determined as a tetragonal structure. At greater depth, SAED analysis reveals a pattern characteristic for a BCC phase. EDS studies performed at points 1 and 2 of Fig. 9, presented in Fig. 10a and Fig. 10b, respectively, illustrate that the tetragonal phase mostly consists of Cr and Co, whereas relatively high peaks for all constituent elements excluding silicon were found in the second structure. High nickel content is especially indicated in Fig. 10b.

XRD results obtained from the surface of the AlCoCrCuNi and AlCoCrCuNi1Si alloys after the high-temperature oxidation at 1273 K for 24 h in air are presented in Fig. 11. From these patterns it follows that the alloys now consist of more phases than simply FCC and BCC. Significant amounts of a tP30 tetragonal structure, recognized in literature as a sigma phase [12-15], form during prolonged exposure to the high temperature. Furthermore, in the case of AlCoCrCuNi, an additional FCC structure was determined, which is in accordance with the combined TEM-SAED

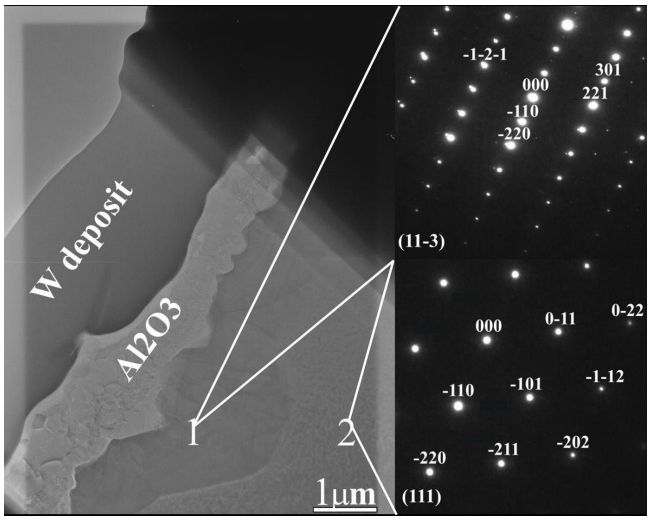

Fig. 9. TEM cross-section image of AlCoCrCuNi1Si after oxidation at 1273 K in air for 24 h combined with SAED patterns obtained from point 1 and point 2 of the microphotograph

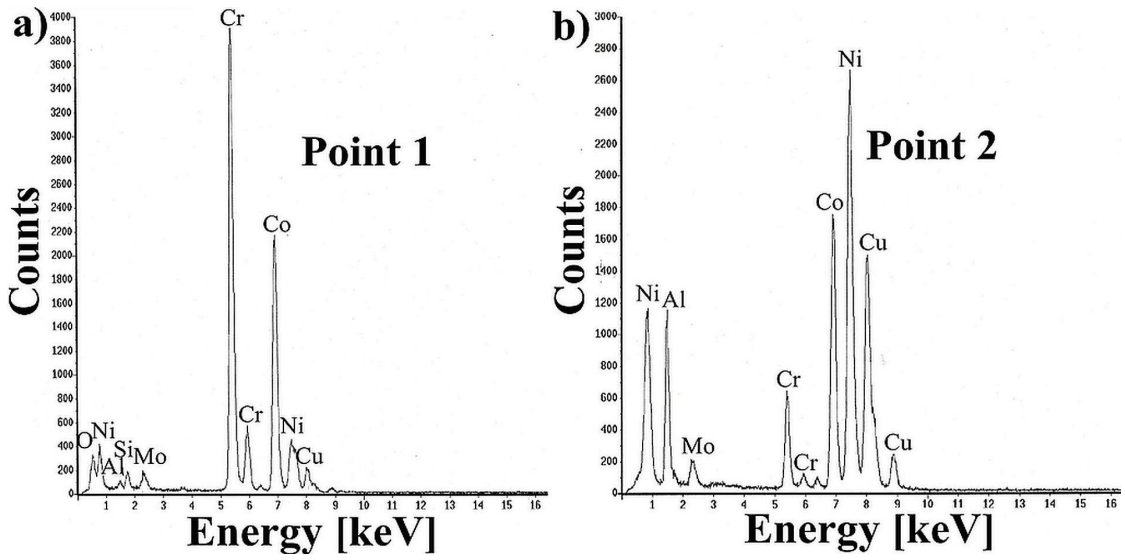

Fig. 10. EDS point analysis obtained from a) point 1 and b) point 2 of the TEM cross-section image of AlCoCrCuNi1Si after oxidation at 1273 K in air for 24 h

analysis carried out in this work on the sample (Fig. 7). Moreover, the formation of α-Al_2O_3 on the surfaces of both HEAs studied in this work was confirmed.

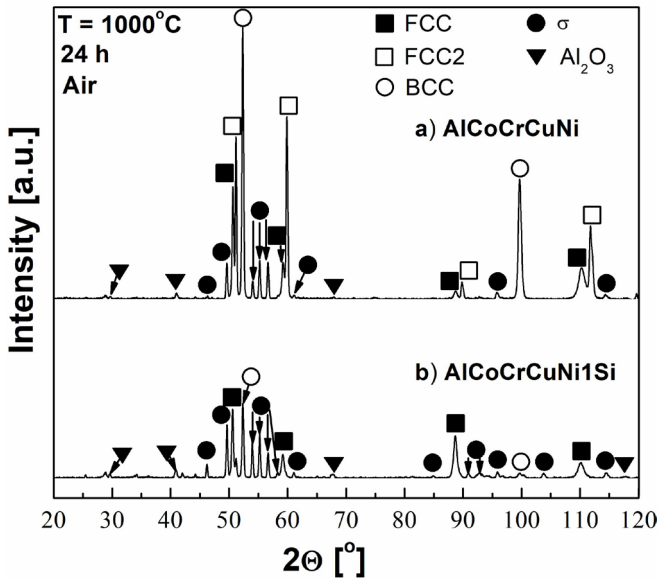

Fig. 11. XRD results obtained from a) AlCoCrCuNi and b) AlCoCrCuNi1Si high entropy alloy after oxidation at 1273 K in air for 24 h

4. Discussion

The results indicate that both AlCoCrCuNi and AlCoCrCuNi1Si materials do not maintain their initial structure after exposure to elevated temperatures. Furthermore, some differences in phase composition were observed in both cases. In the case of AlCoCrCuNi, an additional CoCrNi-rich FCC solid solution was determined near the surface of the sample after oxidation. However, this structure was not observed in the AlCoCrCuNi1Si alloy after exposure to the same conditions. On the other hand, a Cr-Co tetragonal sigma phase, determined by combined TEM-EDS-SAED and XRD analysis, was seen in both samples after exposure to air at 1273 K. This phase has also been observed after heating the AlCoCrCuNi material to temperatures above 873 K in non-oxidizing conditions [12,13]. Therefore, this additional structure formation can be attributed to the influence of high temperature rather than the oxidation process itself. It is interesting to notice that the sigma phase is more prevalent near the surface of the silicon-containing sample compared to the AlCoCrCuNi material. Next to this phase, the initial BCC structure can be found with more significant nickel concentration compared to the other elements. Furthermore, somewhat larger amounts of Cu can be found in the BCC region (Fig. 10b) compared to the CoCrNi FCC phase after oxidation (Fig. 8a). Diffusion behavior of all the individual elements during exposure to high-temperature conditions is still relatively unknown and thus can be the subject of future investigations. Confirming the mechanical properties of the alloys before and after the structural changes, as well as researching ways to eliminate the brittle sigma phase, are also avenues for further research.

From all the combined analysis in this work, the simplified chemical compositions of the phases without impurities, as well as their lattice constants, can be determined. This information is summarized in Table 2.

TABLE 2

Structural information and general compositions of phases detected by XRD analysis of AlCoCrCuNi and AlCoCrCuNi1Si before and after heat treatment at 1273 K in air for 24 h

Designation	Structure	Lattice constant(s) [Å]	Simplified element combination constituting the structure
BCC	Body centered cubic	a ≈ 2.87	Ni-Al-Co-Cr-Cu
FCC	Face centered cubic	a ≈ 3.62	Cu
FCC2	Face centered cubic	a ≈ 3.59	Co-Cr-Ni
σ	Tetragonal tP30	a ≈ 8.81, b = c ≈ 4.56	Cr-Co

As for the oxidation properties determined from these experiments, the lack of a uniform protective scale covering the entire surface of the materials is a significant barrier, which inhibits long-term use and must be overcome if the high entropy alloys are to have practical high-temperature applications. While Al_2O_3 does form on the surfaces, it is only found at certain locations, usually those with lower Cu content. The presence of Cu in the sample contributes to a lack of scale/substrate adherence, according to research carried out by Dabrowa et al. [19], which demonstrates that adhesion between $AlCoCrCu_xFeNi$ high entropy alloys and the Al_2O_3 oxide scale grown on its surface worsens as Cu concentration increases. Taking this into account, it should be possible to improve oxidation properties by removing Cu from the system. This work also demonstrates that even minor silicon addition (1 at.%) can affect the phase composition of the alloy after prolonged exposure to oxidizing conditions at a high temperature. However, it is important to be careful before incorporating high concentrations of Si into the AlCoCrCuNi system due to the possibility of additional intermetallic phase formation. Thus, research on determining an optimum Si content should be carried out in future studies.

5. Conclusions

From all the obtained results, the following can be concluded:

- Oxidation of AlCoCrCuNi high entropy alloys at elevated temperatures is a very complex process that leads to the formation of additional structures both in the materials and on their surfaces;
- The phase composition at high temperature and oxidation kinetics of AlCoCrCuNi are affected by minor amounts of silicon in the system;

- The Al_2O_3 scale formed during prolonged exposure of the AlCoCrCuNi samples to oxidizing conditions at high temperatures does not ensure uniform protection for the alloys.

Acknowledgements

The authors are grateful for financial support from Iketani Science and Technology foundation, as well as the Center for Advanced Materials Research and International Collaboration (CAMRIC) and University of Toyama.

REFERENCES

[1] J.-W. Yeh, S.-K. Chen, S.-J. Lin, J.-Y. Gan, T.-S. Chin, T.-T. Shun, C.-H. Tsau, S.-Y. Chang, Adv. Eng. Mater. **6** (5), 299-303 (2004).

[2] D.B. Miracle, J.D. Miller, O.N. Senkov, C. Woodward, M.D. Uchic, J. Tiley, Entropy **16**, 494-525 (2014).

[3] A. Gali, E.P. George, Intermetallics **39**, 74-78 (2013).

[4] B. Gludovatz, A. Hohenwarter, D. Catoor, E.H. Chang, E.P. George, R.O. Ritchie, Science **345**, 1153-1158 (2014).

[5] Y.P. Wang, B.S. Li, M.X. Ren, C. Yang, H.Z. Fu, Mater. Sci. Eng. A **491**, 154-158 (2008).

[6] C.-J. Tong, Y.-L. Chen, S.-K. Chen, J.-W. Yeh, T.-T. Shun, C.-H. Tsau, S.-J. Lin, S.-Y. Chang, Metall. Mater. Trans. A **36A**, 881-893 (2005).

[7] W.-R. Wang, W.-L. Wang, S.-C. Wang, Y.-C. Tsai, C.-H. Lai, J.-W. Yeh, Intermetallics **26**, 44-51 (2012).

[8] J.Y. He, W.H. Liu, H. Wang, Y. Wu, X.J. Liu, T.G. Nieh, Z.P. Lu, Acta Mater. **62**, 105-113 (2014).

[9] J.M. Zhu, H.M. Fu, H.F. Zhang, A.M. Wang, H. Li, Z.Q. Hu, Mater. Sci. Eng. A **527**, 7210-7214 (2010).

[10] C.-C. Yang, J.L.H. Chau, C.-J. Weng, C.-S. Chen, Y.-H. Chou, Mat. Chem. Phys. **202**, 151-158 (2017).

[11] U.S. Hsu, U.D. Hung, J.W. Yeh, S.K. Chen, Y.S. Huang, C.C. Yang, Mater. Sci. Eng. A **460-461**, 403-408 (2007).

[12] Ł. Rogal, Mater. Sci. Eng. A **709**, 139-151 (2018).

[13] Ł. Rogal, J. Morgiel, F. Stein, B. Breitbach, J. Dutkiewicz, Mat. Char. **148**, 134-141 (2019).

[14] M.-H. Tsai, H. Yuan, G. Cheng, W. Xu, W.W. Jian, M.-H. Chuang, C.-C. Juan, A.-C. Yeh, S.-J. Lin, Y. Zhu, Intermetallics **33**, 81-86 (2013).

[15] M.-H. Tsai, K.-C. Chang, J.-H. Li, R.-C. Tsai, A.-H. Cheng, Mater. Res. Lett. **4** (2), 90-95 (2016).

[16] T.M. Butler, M.L. Weaver, J. Alloys Compd. **674**, 229-244 (2016).

[17] T.M. Butler, J.P. Alfano, R.L. Martens, M.L. Weaver, JOM **16**, 246-259 (2015).

[18] Y.Y. Liu, Z. Chen, Y.Z. Chen, J.C. Shi, Z.Y. Wang, S. Wang, F. Liu, Vacuum **169**, 108837 (2019).

[19] J. Dąbrowa, G. Cieślak, M. Stygar, K. Mroczka, K. Berent, T. Kulik, M. Danielewski Intermetallics **84**, 52-61 (2017).

[20] Ł. Rogal, J. Morgiel, Z. Świątek, F. Czerwiński, Mater. Sci. Eng. A **651**, 590-597 (2016).